Clin Transl Oncol (2017) 19:641–649
DOI 10.1007/s12094-016-1580-3

RESEARCH ARTICLE

Imaging findings of adrenal primitive neuroectodermal tumors: a series of seven cases

Y. Zhang[1] · P. Cai[2] · M. Chen[3] · X. Yi[1] · L. Li[2] · D. Xiao[4] · W. Liu[1] · W. Li[1] · Y. Li[5]

Received: 12 July 2016 / Accepted: 12 November 2016 / Published online: 23 November 2016

Abstract
Objective To explore the imaging features of adrenal primitive neuroectodermal tumors (PNETs).
Materials and methods This retrospective study included seven patients with surgically and pathologically confirmed adrenal PNETs. Among them, six underwent computed tomography (CT) scans, and one underwent magnetic resonance imaging. The imaging findings, including size, shape, margin, hemorrhage, calcification, cystic degeneration, regional lymph nodes involvement, tumor thrombus formation and enhancement pattern, were retrospectively analyzed.
Results Among the seven adrenal PNET patients, six were male, and one was female. The median age was 26 years (range 2–56 years). The disease generally presented with either insidious symptoms ($n = 4$) or non-specific symptoms, including right flank pain ($n = 1$) and left upper abdominal discomfort ($n = 2$). On the pre-enhanced CT images, the tumor usually appeared as a well-defined, rounded or oval, heterogeneous mass without calcification. Certain tissue characteristics, such as cystic degeneration ($n = 5$), capsule ($n = 4$) and hemorrhage ($n = 2$), were observed. Regional lymph node involvement was observed in three cases, and renal vein thrombus was observed in one case. All cases showed mild heterogeneous enhancement of the tumor on the enhanced CT images.
Conclusion An adrenal PNET commonly presents as a relatively large, well-defined, heterogeneous mass with cystic degeneration, necrosis and a characteristic mild contrast-enhancement pattern on multiphase enhanced images. PNET should be considered when the diagnosis of common tumors is not favored by signs on images.
Clinical Trial Registration Statement This study was approved by the medical ethics committee of Xiangya Hospital, Central South University. The approval number is 201512538.

Keywords Primitive neuroectodermal tumors (PNETs) · Computed tomography (CT) · Magnetic resonance imaging (MRI) · Adrenal tumors · Diagnosis

Y. Zhang, P. Cai and M. Chen contributed equally to this work.

✉ X. Yi
doctoryixiaoping@126.com

[1] Department of Radiology, Xiangya Hospital, Central South University, 87# XiangYa Road, Changsha 410008, Hunan, People's Republic of China

[2] Imaging Diagnosis and Interventional Center, Sun Yat-sen University Cancer Center, Guangzhou, People's Republic of China

[3] Department of Ultrasonography, Xiangya Hospital, Central South University, Hunan, People's Republic of China

[4] Department of Pathology, Xiangya Hospital, Central South University, Hunan, People's Republic of China

[5] Departments of General Surgery, Xiangya Hospital, Central South University, Hunan, People's Republic of China

Introduction

Primary neuroectodermal tumors (PNETs), which are part of the Ewing's sarcoma (EWS) family of tumors, are highly malignant tumors comprising small round cells with a neuroectodermal origin and occur primarily in children and adolescents. PNETs are divided into two types based on the location in the body: central primary neuroectodermal tumors [1] and peripheral primitive neuroectodermal tumors (pPNETs) [2]. pPNETs have a predilection for the chest wall (Askin's tumor), trunk and lower extremities

[3–5]. PNETs have rarely been reported in the head and neck, spinal column or retroperitoneum (kidney, pancreas and uterus) [5–8]. PNETs presenting in the adrenal gland show a correspondence in age with adrenocortical carcinoma and malignant pheochromocytoma, and all these tumors are extremely rare.

Approximately 21 cases of adrenal PNETs have been reported in the literature, and most of those studies are case reports. The imaging characteristics of adrenal PNETs are largely unknown [9–13]. It is easy to misdiagnose PNET as another disease arising from the adrenal glands or the retroperitoneal organs during clinical practice. In addition, a timely and accurate preoperative diagnosis of an adrenal tumor as a PNET may be particularly important because of its high rate of malignancy and early metastasis [14]. Here, we conducted a retrospective study to describe the imaging features of this disease to improve preoperative diagnosis of PNET.

Materials and methods

Design and patients

This retrospective study was approved by the hospital's Institutional Review Board. Written or verbal informed consent was obtained from all patients. From January 2005 to April 2016, seven patients at our hospital were surgically and pathologically confirmed to have primary adrenal PNETs. Based on their financial situations, six underwent complete computed tomography (CT) scans, and one underwent a magnetic resonance imaging (MRI) examination. The clinical and radiological data were collected.

CT and MR imaging

The CT examination was performed with a 320-detector volume CT system (Aquilion ONE, Toshiba, Japan) or a Somatom Definition dual-source CT (DSCT, Siemens Medical System, Forchheim, Germany). The scan parameters were as follows: 5-mm section thickness, 1-mm slice thickness reconstructions, 120-kV voltage, 90- to 270-mA current, and 256 × 256 matrix. A 100-mL intravenous bolus dose of a non-ionic iodinated contrast agent (iopromide; Ultravist; Schering AG, Berlin, Germany) was administered at a rate of 3–4 mL/s. MR images were obtained with a 1.5-T superconductive unit (Singa HD xt, GE Medical Systems, United States), and an abdominal coil was used. The sequences included coronal turbo spin echo T2-weighted images and transverse T1-/T2- and diffusion-weighted images. The parameters of these sequences were repetition time (TR)/echo time (TE) = 4/1.8 ms for coronal T2-weighted images; TR/TE = 165/1.3 ms for transverse T1-weighted images; TR/TE = 9230/92 ms for transverse T2-weighted images; TR/TE = 5000/69 ms for diffusion-weighted images; fields of view of 65 × 65 for transverse images and 100 × 100 for coronal images; a matrix of 512 × 512; 4–6 signal acquisition; and a slice thickness/gap of 3/0.3 mm. Contrast-enhanced coronal and transverse T1-weighted images were obtained after an intravenous injection of gadopentetate dimeglumine (Magnevist, Schering, Berlin, Germany) at a dose of 0.2 mmol/kg at a rate of 1.5 mL/s.

Imaging analysis

Three radiologists specializing in abdominal diseases independently evaluated CT and MRI features of the imaging data, including size, shape, margin, hemorrhage, calcification, attenuation/signal, regional lymph nodes, thrombus, and enhancement features after the intravenous contrast medium injection, and disagreements were resolved by consensus. Areas of suspected hemorrhage were analyzed when the CT attenuation values fell in the range of 50–90 Hu on unenhanced scans [15, 16] or in cases of short T1- and long T2-signal changes on the MR images. Data analysis of CT images was performed based on regions of interest (ROIs). Each ROI was drawn manually on the solid parts three times, and the average CT attenuation was then calculated.

Results

Clinical data

The six men and one woman in this study had a median age of 26 years (range 2–56 years). The clinical symptoms that contributed to the diagnosis were diverse and non-specific, and included left upper abdominal discomfort ($n = 2$, 28.6%); right flank pain ($n = 1$, 14.3%); and incidental findings ($n = 4$, 57.1%). The duration of symptoms varied from 2 days to 1 month. Laboratory results showed no evidence of hormonal hypersecretion (vanillylmandelic acid, 17-hydroxycorticosteroids, 17-ketosteroids) in four patients, one of whom had a high level of neuron-specific enolase (NSE) (greater than 370 ng/mL).

Imaging findings

The imaging findings of the seven adrenal PNET cases are shown in Table 1. Each case exhibited a single tumor for a total of seven tumors. Of these, six (6/7, 85.7%) were located on the left adrenal gland, and the remaining one (1/7, 14.3%) was on the right side. All tumors were well defined. The mean long diameter of the tumors was

7.24 cm. The tumors were round in five (5/7, 71.4%) cases and oval in two (2/7, 28.6%) cases. Among the seven patients, cystic degeneration was observed in five (5/7, 71.4%) (Figs. 1, 2, 3, 4, 5, 6). Capsule was observed in four (4/7, 57.1%) cases, and hemorrhage was observed in two (2/7, 28.6%) cases (Figs. 2, 6). No calcifications were observed. Regional lymph node involvement was observed in three (3/7, 42.9%) cases (Fig. 1, 6), and renal vein thrombus was observed in one (1/7, 14.3%) case (Fig. 2).

The tumors showed mild heterogeneous enhancement patterns on the contrast-enhanced CT images (Figs. 1, 2, 3, 4, 5, 6), with mean CT attenuations of 47.9 Hu (range 43.6–52.8 Hu) on the pre-enhanced CT images, 56.8 Hu (range 52.2–66.1 Hu) in the arterial phase, and 64.5 Hu

Table 1 The imaging features of seven cases with adrenal PNET

Case	Sex/age (years)	L/R	CT/MRI	D (cm)	Shape	Margin	Septation	Cys	Hem	Cal	Enhancement pattern	LN	Embolus
1	M/12	R	CT	5.4	Round	Well-defined	−	+	−	−	Mild, heterogeneous enhancement	+	−
2	M/27	L	CT	6.4	Round	Well-defined	−	−	+	−	Mild, heterogeneous enhancement	−	+
3	M/2	L	CT	3.2	Round	Well-defined	−	−	−	−	Mild, heterogeneous enhancement	+	−
4	M/48	R	CT	7.7	Oval	Well-defined	−	+	−	−	Mild, heterogeneous enhancement	−	−
5	M/22	L	CT	8.8	Oval	Well-defined	−	+	−	−	Mild, heterogeneous enhancement	−	−
6	F/56	L	CT	11.6	Round	Well-defined	−	+	−	−	Mild, heterogeneous enhancement	−	−
7	M/36	L	MRI	7.6	Round	Well-defined	–	+	+	−	Mild, heterogeneous enhancement	+	−

M male, *F* female, *D* diameter, *Cys* cystic degeneration, *Hem* hemorrhage, *Cal* calcification, *LN* lymph nodes involvement

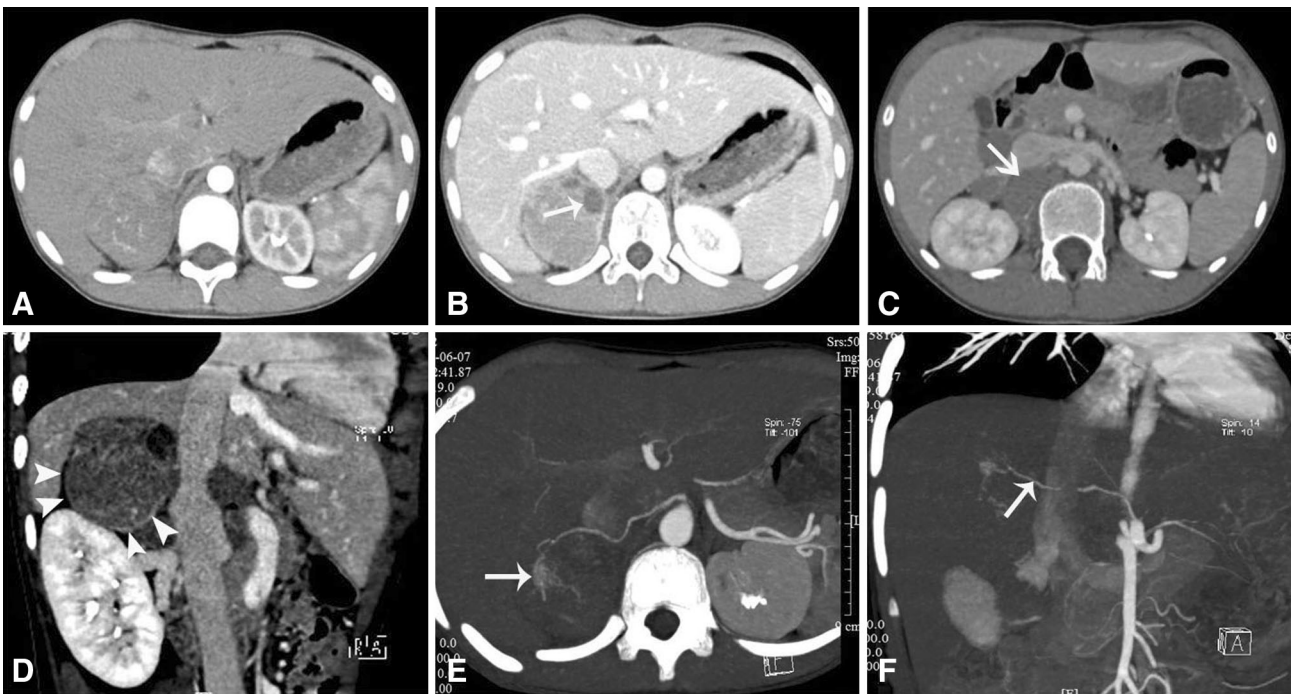

Fig. 1 CT findings of a 12-year-old man with an adrenal PNET (case 1). The enhanced CT images showed a well-defined, rounded, solid mass in the region of the right adrenal gland (**a**, **b**). The tumor displayed mild heterogeneous enhancement in the arterial and venous phases (**a**, **b**) with patchy cystic degeneration areas (**b** *arrow*). Regional lymph node involvement was observed surrounding the inferior vena cava and right renal vessels (**c** *arrow*). Thin rim enhancement was displayed (**d** *arrowheads*). The neovascularization within the tumor was clearly noted on CTA (**e** *arrow*) and by the blood supply to the tumor from the coeliac trunk (**f** *arrow*)

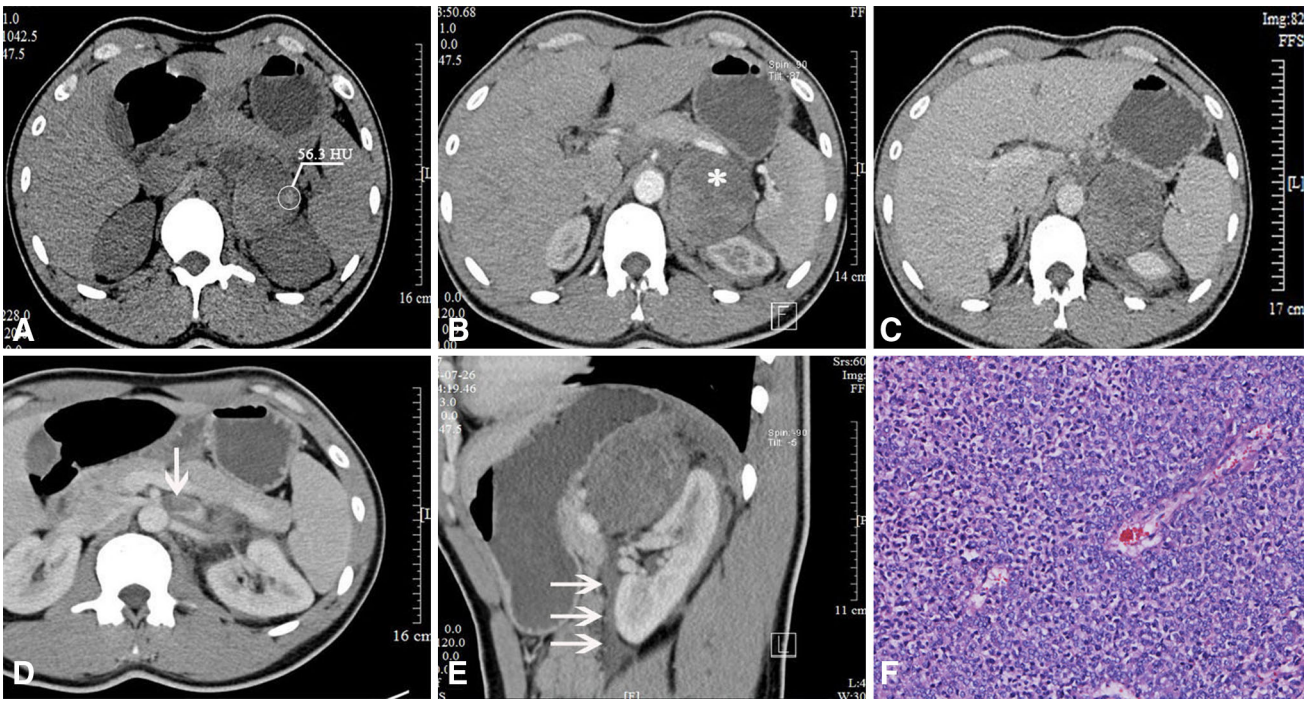

Fig. 2 CT findings of a 27-year-old man with an adrenal PNET (case 2). Pre-enhanced CT images showed a well-defined, rounded, soft-density mass on the left adrenal gland. Patchy areas of hemorrhage were observed with a CT value of 56.3 Hu (**a**). A patchy low attenuation area was observed in the tumor (**b**) (*asterisk*). The mass showed mild heterogeneous enhancement (**b**, **c**). Left renal vein thrombus was observed (**d**, *arrow*). An area of fluid attenuation surrounding the left renal area was present (**e** *arrows*)

(range 53.2–82.9 Hu) in the venous phase. Thin rim enhancement and neovascularization of the masses were observed in four (4/7, 57.1%) patients (Fig. 1, 3, 5, 6) and one patient (Fig. 1), respectively.

Surgical and pathological findings

All patients underwent an adrenalectomy, and all tumors originated from the adrenal glands. The tumors appeared as soft, well-circumscribed oval or rounded masses with a tan-yellow appearance. All tumors were heterogeneous in texture, particularly the larger tumors. Cystic degeneration, necrosis ($n = 5$) and hemorrhage ($n = 2$) were observed.

Hematoxylin and eosin staining showed that the adrenal medulla was completely replaced by a malignant tumor comprising small, round cells arranged in cords or rosettes (Figs. 2, 3) with a compressed rim of the adrenal cortex at the periphery. Immunohistochemical staining (Table 2) revealed that six (6/7, 85.7%) tumors were positive for CD99; six (6/7, 85.7%) were positive for vimentin; four (4/7, 57.1%) were positive for NSE, five (5/7, 71.4%) were positive for synaptophysin (Syn), and five (5/7, 71.4%) were positive for S-100 protein. The Ki67 index in the seven cases varied from approximately 30 to 90%, indicating that the tumors had high proliferation activity.

Discussion

PNET and EWS are considered to be two stages of the same tumoral entity, and they share a unique and specific *t*(11;22)(q24;q12) chromosomal translocation, although they can be distinguished by the presence or absence of neural differentiation. The immunohistochemical markers of neuroepithelial differentiation, such as CD99, vimentin, NSE, Syn, and S-100 protein, are frequently positive in PNETs but not in EWS [17]. Pathological diagnosis of PNET depends on the presence of rosettes and pseudorosettes consisting of small and round cells, and two or more positive neural markers.

Primary adrenal PNETs are extremely rare. The adrenal medulla originates from embryonic neural crest. From this perspective, PNET may have histological origin in the adrenal gland. Similar to other reports [9–13], the adrenal PNET patients in our study all tended to present with insidious or non-specific symptoms, such as abdominal or flank pain, that were likely secondary to the compression effect of the tumor.

In this study, all seven masses were relatively large, with a mean diameter of 7.6 cm. This may be due to the fact that the retroperitoneal space surrounding the adrenal glands is relatively large, and tumors growing in the adrenal region are less palpable through the body surface. Therefore, they

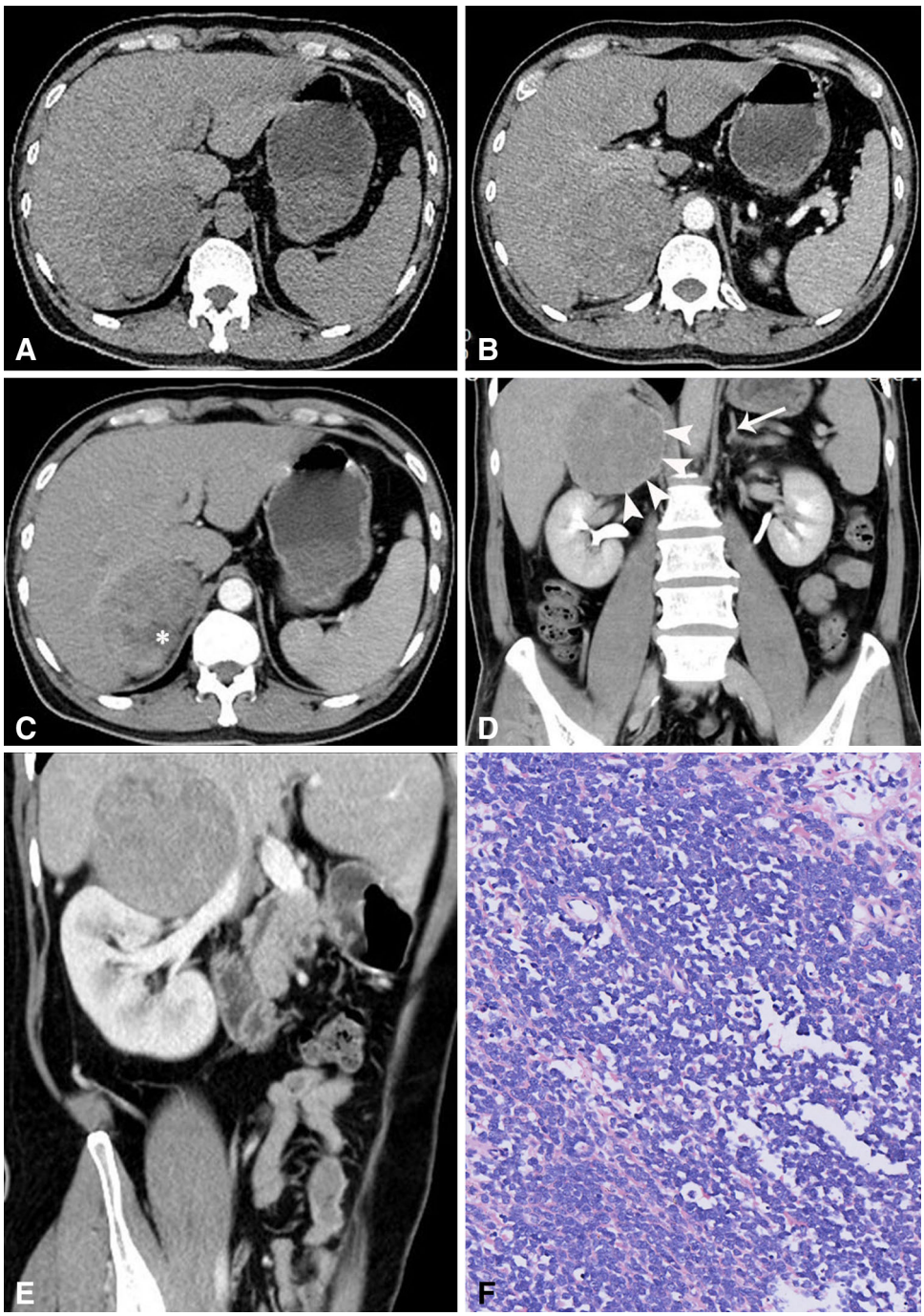

Fig. 3 An adrenal PNET in a 48-year-old man (case 4) (**a**–**e**). The mass was well defined and rounded and was found in the region of the right adrenal gland. A contrast-enhanced CT image showed mild heterogeneous enhancement (**b**, **c**) with patchy cystic degeneration areas (**c** *asterisk*). Thin rim enhancement was displayed (**d** *arrowheads*), and the left adrenal gland appeared to be normal (**d** *arrow*). The right renal area was compressed in the oblique sagittal position (**e**)

are likely to be discovered only after they have become enlarged. This also explains why indolent enlargement of the mass is presumed to be primary clinical manifestation. In addition, symptoms generally do not appear until the displacement of the kidney or other adjacent organs becomes overt.

The tumors in this study were solitary rounded and oval masses with well-defined margins and a complete capsule on CT/MR images, consistent with previous reports that adrenal PNETs usually appear as unilateral, rounded or oval solitary masses with well-defined margins [12, 13]. In addition, a well-defined capsule and thin rim enhancement were observed in 57.1% (4/7) of patients. This may suggest an expansive rather than an infiltrative growth pattern because most benign tumors are well-defined encapsulated masses [18]. However, a complete capsule does not absolutely indicate an early-stage tumor with benign biological behavior. In malignant tumors, rapid growth of the tumor cells leads to a rapid increase in tumor volume and suppression of the surrounding

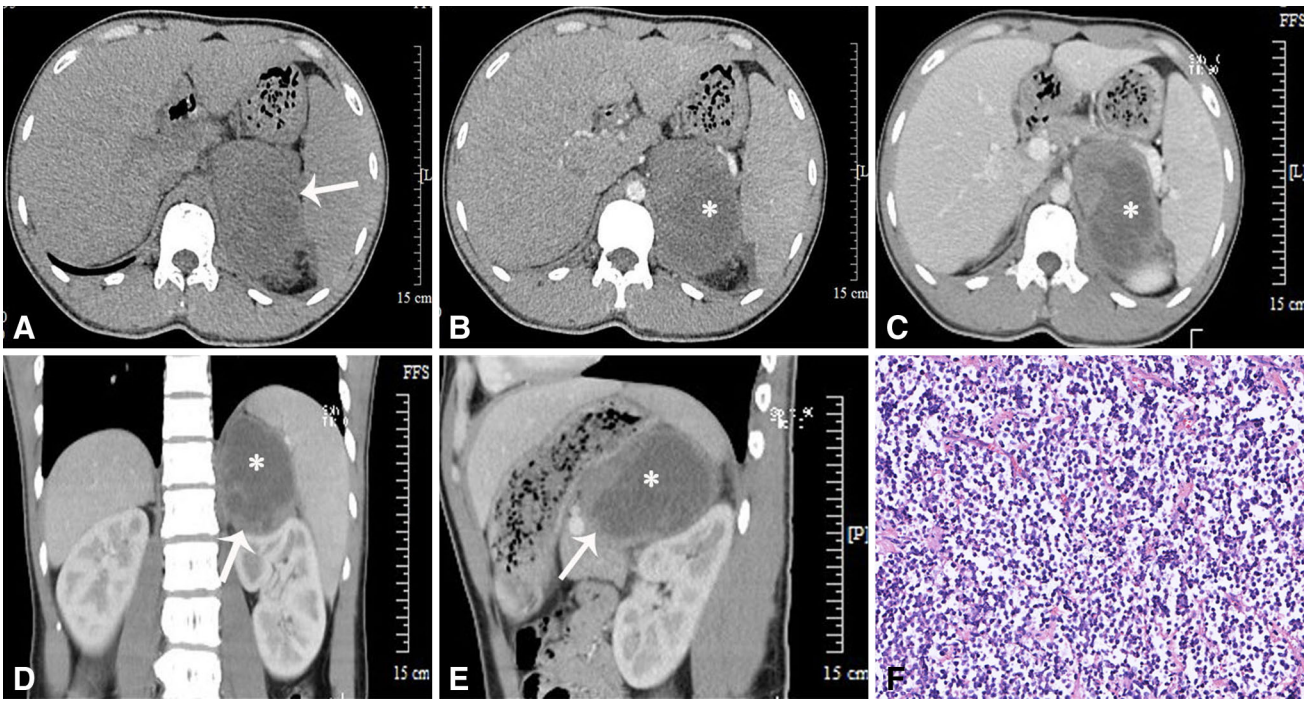

Fig. 4 An adrenal PNET in a 22-year-old man (case 5) (**a**–**e**). An unenhanced CT scan showed a well-defined oval mass in the region of the left adrenal gland. The mass showed mild heterogeneous enhancement with patchy cystic degeneration areas (**b**–**e** *asterisks*). The left renal area was compressed in the coronal and sagittal positions (**d**, **e** *arrows*)

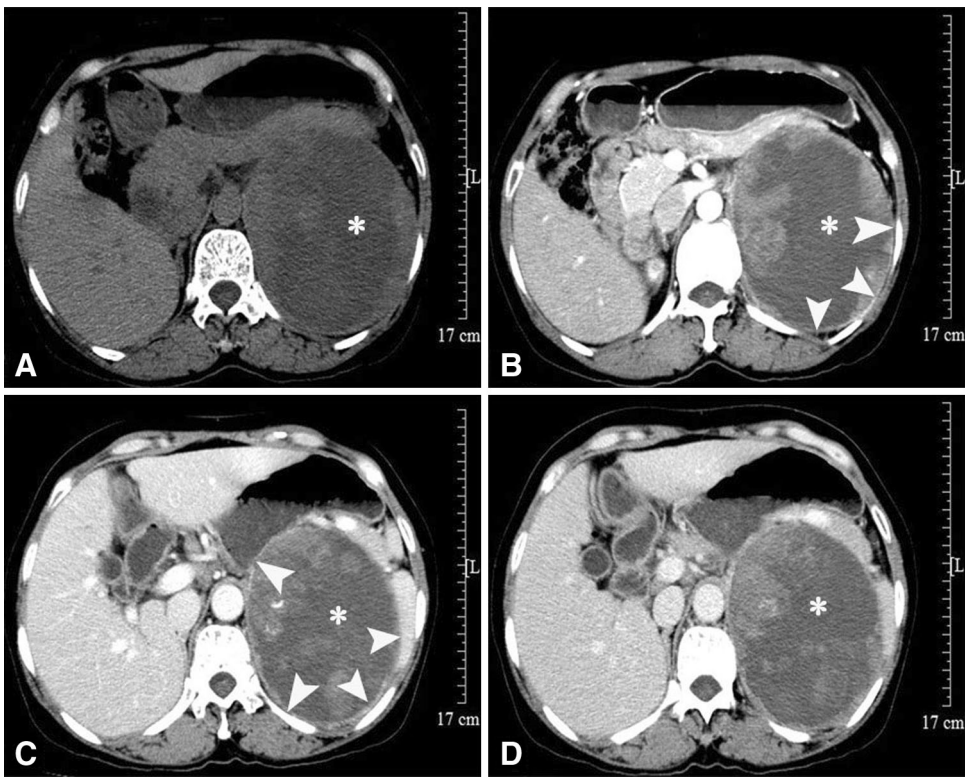

Fig. 5 An adrenal PNET in a 56-year-old woman (case 6) (**a**–**d**). An unenhanced CT scan showed a well-defined rounded mass in the region of the left adrenal gland. The mass showed mild heterogeneous enhancement with large patchy cystic degeneration areas (**b**–**d** *asterisks*). Thin rim enhancement was displayed (**c** *arrowheads*)

connective and fibrous tissues, which in turn results in the formation of a "false capsule" and a well-defined tumor margin. Therefore, this context may represent a rapid growth pattern of tumor cells, but it does not mean that a tumor is non-invasive. The adrenal PNET may be such an example.

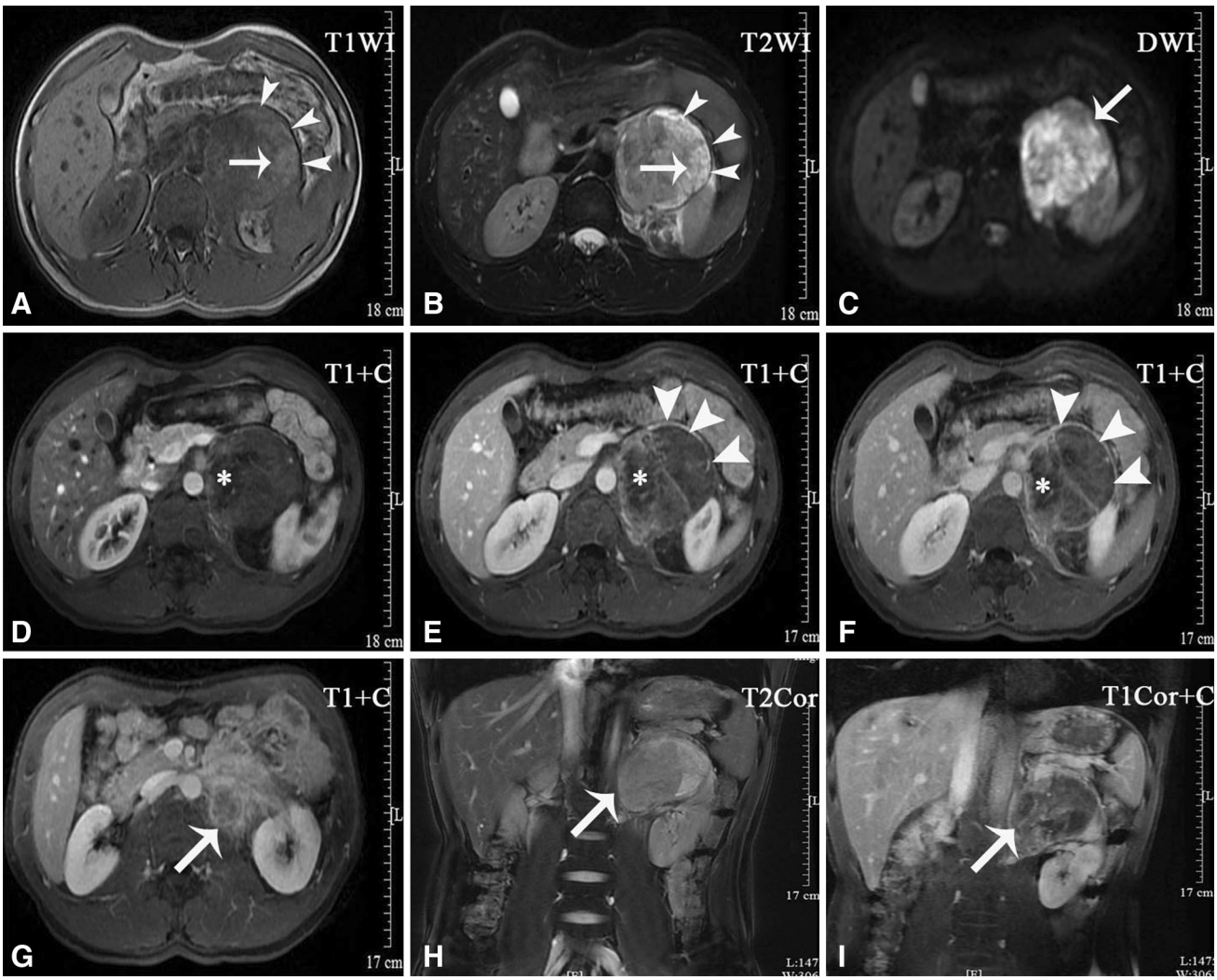

Fig. 6 MRI findings of a 36-year-old man (case 7) with an adrenal PNET in the region of the left adrenal gland (**a**–**i**). The signal intensity of the tumor was heterogeneous and slightly hypointense and hyperintense on the T1- and T2-weighted images, respectively (**a**, **b**). A patchy abnormal signal area within the tumor with a hyperintense signal on both T1- and T2-weighted images was observed, indicating hemorrhage (**a**, **b** *arrows*). Diffusion-weighted images showed hyperintense signals (**c**). The mass showed mild heterogeneous enhancement with patchy cystic degeneration areas (**d**–**f** *asterisks*). Thin rim enhancement was displayed (**e**, **f** *arrowheads*). Regional lymph node involvement was observed surrounding the left renal vessels (**g** *arrow*). The left renal area was compressed in the coronal position (**h**, **i** *arrows*)

Calcification is uncommon in PNETs [18, 19]. Li et al. reported calcification in only 1 of 12 PNETs in the abdominopelvic region [18], while Xu et al. reported that none of the PNETs among 14 patients was positive for calcification [17]. In our study, we did not observe calcification in any of the seven tumors by CT/MRI scans. In addition, hemorrhage was found in 28.6% (2/7) of the patients in this study. Among those, one presented with patchy, high-density areas with an average CT attenuation value of 56.3 Hu, and the other showed hyperintense signals on both T1- and T2-weighted images.

Consistent with previous studies [20, 21], the adrenal PNET cases in this study appeared as heterogeneous, soft-tissue density/signal masses with patchy fluid attenuation areas and mild heterogeneous enhancement. Notably, degenerative changes, such as cystic degeneration and necrosis, were secondary due to an inadequate blood supply to the corresponding region in the tumor. Microscopically, the tumor comprised sparsely scattered stromal elements and a large number of compactly arranged, small, blue, round cells, which appeared to be uniform and had ovoid hyperchromatic irregular nuclei and scant cytoplasms [13]. Because dense tumor cells occupy a significant amount of space, the proportion of stromal elements such as blood vessels is relatively small. This may partially explain the relatively weak enhancement of tumors on the enhanced images.

Table 2 Immunohistochemistry features of seven adrenal PNET

Case	Positive	Negative
1	CgA,NSE, Syn, Vim	CD99, CK-pan, EMA, CK5/6, P63
2	CD99, Vim, Syn, S100, NSE	CD10, CD5, CK-pan, CgA, EMA, HHF35, LCA, Bcl-2, CD20, CD3, CD30, CD43, CD45RO, CK-l, CXCL-13, HMB45, Melan-A, PAX-5
3	CD99, Vim, S100, Syn	CD10, CD20, CD3, CD56, CD79a, CK-pan, EMA, Myogenin, PAX-5, TdT, MPO, CgA
4	CD99, CD56, S100, Syn, Nestin	CgA, CK-pan, NF-pan, NSE
5	NSE, Syn, CD99	CgA, CD56, Vim, CK, CK7, TTF1, CD10, WT-1, CK5/6, EMA, Des, GFAP, HHF35, CD34
6	NSE, S100, CgA, Des, HHF35, Myo, Vim, EMA, CD99, CD56	CK, CD10, L26, CD79a, CD3, LCA, PLAP, CK-L, ALK, CD30
7	CD56, Syn, NSE, CD99, Vim	CK, EMA, CgA, LCA, CD20, CD3, WT-1, Des, Myogenin, Neu-N, CD34, Dog-1, NF, GFAP

Because of the high malignancy and invasiveness of PNETs, they often demonstrate regional lymph node involvement, distant metastases and local recurrence after treatment [6, 17, 18]. In our study, regional lymph node involvement was observed in 42.9% (3/7) of patients, and renal vein tumor embolus and local recurrence were found in one patient, respectively. To avoid unnecessary injury during surgery, it is very important to recognize the vessels supplying the adrenal tumors prior to surgery. CT angiography (CTA) techniques are very effective at displaying tumor-feeding vessels. In our study, one patient underwent a CTA examination. The tumor-feeding artery originated from the coeliac trunk, and neovascularization within the tumor was clearly presented on the CTA images.

The differential diagnosis of an adrenal PNET involves a variety of tumors that primarily include nonfunctioning benign or malignant tumors. As the most common type of adrenal tumor, a lipid-rich adenoma is easy to exclude based on its characteristic attenuation value of less than 10 Hu on pre-enhanced CT images [16]. Lipid-poor adenomas can be differentiated from non-adenomas by the characteristic rapid washout of contrast materials in delayed-phase images [16, 22]. Adrenal ganglioneuromas always present as homogenous, well-defined oval, crescentic or lobulated masses with slight to moderate enhancement. An adrenal schwannoma usually appears as a well-defined rounded or oval solid or cystic mass with septation and progressive contrast enhancement [23]. An adrenal abscess should be considered when a patient presents with fever and immune system disorders, rapid growth, and colliquation transformation [23].

Malignant adrenal tumors, such as adrenocortical carcinoma, pheochromocytoma and adrenal metastasis, should also be differentiated from adrenal PNETs. Adrenocortical carcinoma is rare and is characterized by a large (>6 cm in diameter) infiltrative growth, local invasion, and distant metastasis [24]. Unlike an adrenal PNET, a malignant pheochromocytoma is characterized by heterogeneously marked enhancement. Adrenal metastases are common in the unilateral or bilateral adrenal glands. A history of malignancy plays an important role in the diagnosis of adrenal metastases, which typically present as homogeneous, round, soft-tissue masses when the tumor is relatively small and heterogeneous masses with a thick enhancing rim in larger tumors [10, 23, 24].

Conclusion

In summary, primary adrenal PNETs are extremely rare and difficult to diagnose preoperatively. Some imaging features may be suggestive of the diagnosis of an adrenal PNET. Generally, when a well-defined, unilateral, rounded or oval, relatively large soft-density adrenal mass with mild heterogeneous enhancement is encountered incidentally, and the diagnosis of a common tumor is not supported by radiological signs on CT/MR images, the possibility of a PNET should be considered preoperatively.

Acknowledgements This study was supported by the Freedom Exploration Program of Central South University (No. 2011QNZT153) and Natural Science Foundation of Hunan Province (No. 14JJ6001).

Compliance with ethical standards

Ethical standards This study was conducted in accordance with the Declaration of Helsinki, all its amendments, and national regulations. This retrospective study was approved by the hospital's Institutional Review Board. Written or verbal informed consent was obtained from all patients.

Conflict of interest None of the authors has declared any conflict of interest.

References

1. Biegel JA, Rorke LB, Packer RJ, Sutton LN, Schut L, Bonner K, et al. Isochromosome 17q in primitive neuroectodermal tumors of the central nervous system. Genes Chromosomes Cancer. 1989;1:139–47.
2. Dehner LP. Peripheral and central primitive neuroectodermal tumors. A nosologic concept seeking a consensus. Arch Pathol Lab Med. 1986;110:997–1005.

3. Kushner BH, Hajdu SI, Gulati SC, Erlandson RA, Exelby PR, Lieberman PH. Extracranial primitive neuroectodermal tumors. The Memorial Sloan-Kettering Cancer Center experience. Cancer. 1991;67:1825–9.
4. Hari S, Jain TP, Thulkar S, Bakhshi S. Imaging features of peripheral primitive neuroectodermal tumours. Br J Radiol. 2008;81:975–83.
5. Jürgens H, Bier V, Harms D, Beck J, Brandeis W, Etspüler G, et al. Malignant peripheral neuroectodermal tumors. A retrospective analysis of 42 patients. Cancer. 1988;61:349–57.
6. Duan XH, Ban XH, Liu B, Zhong XM, Guo RM, Zhang F, et al. Intraspinal primitive neuroectodermal tumor: imaging findings in six cases. Eur J Radiol. 2011;80:426–31.
7. Mandal PK, Mukherjee S, Roy S, Bhattacharyya NK. PNET of kidney: report of four cases. Indian J Med Paediatr Oncol. 2012;33:130–3.
8. Karpate A, Menon S, Basak R, Yuvaraja TB, Tongaonkar HB, Desai SB. Ewing sarcoma/primitive neuroectodermal tumor of the kidney: clinicopathologic analysis of 34 cases. Ann Diagn Pathol. 2012;16:267–74.
9. Dutta D, Shivaprasad KS, Das RN, Ghosh S, Chowdhury S. Primitive neuroectodermal tumor of adrenal: clinical presentation and outcomes. J Cancer Res Ther. 2013;9:709–11.
10. Yoon JH, Kim H, Lee JW, Kang HJ, Park HJ, Park KD, et al. Ahn, Ewing sarcoma/peripheral primitive neuroectodermal tumor in the adrenal gland of an adolescent: a case report and review of the literature. J Pediatr Hematol Oncol. 2014;36:e456–9.
11. Sasaki T, Onishi T, Yabana T, Hoshina A. Ewing's sarcoma/primitive neuroectodermal tumor arising from the adrenal gland: a case report and literature review. Tumori. 2013;99:e104–6.
12. Abi-Raad R, Manetti GJ, Colberg JW, Hornick JL, Shah JG, Prasad ML. Ewing sarcoma/primitive neuroectodermal tumor arising in the adrenal gland. Pathol Int. 2013;63:283–6.
13. Zhang L, Yao M, Hisaoka M, Sasano H, Gao H, Zhang Y, et al. Primary Ewing sarcoma/primitive neuroectodermal tumor in the adrenal gland. APMIS. 2016;. doi:10.1111/apm.12544.
14. Teixeira U, Goldoni M, Unterleider M, Diedrich J, Balbinot D, Rodrigues P, Fontes F Waechter, et al. Primitive neuroectodermal tumor of the pancreas: a case report and review of the literature. Case Rep Surg. 2015;2015:276869.
15. Dunnick NR. Hanson lecture. Adrenal imaging: current status. AJR Am J Roentgenol. 1990;154:927–36.
16. Taffel M, Haji-Momenian S, Nikolaidis P, Miller FH. Adrenal imaging: a comprehensive review. Radiol Clin N Am. 2012;50:219–43.
17. Qian X, Kai X, Shaodong L, Gaohong C, Hong M, Jingjing L. Radiological and clinicopathological features of pPNET. Eur J Radiol. 2013;82:e888–93.
18. Li X, Zhang W, Song T, Sun C, Shen Y. Primitive neuroectodermal tumor arising in the abdominopelvic region: CT features and pathology characteristics. Abdom Imaging. 2011;36:590–5.
19. Dick EA, Mchugh K, Kimber C, Michalski A. Imaging of non-central nervous system primitive neuroectodermal tumours: diagnostic features and correlation with outcome. Clin Radiol. 2001;56:206–15.
20. Gong J, Zhang Y, Zuo M, Yang Z, Zang D, Bao S, et al. Imaging findings of abdominal peripheral primitive neuroectodermal tumor: report of four cases with pathological correlation. Clin Imaging. 2009;33:196–9.
21. Ba L, Tan H, Xiao H, Guan Y, Gao J, Gao X. Radiologic and clinicopathologic findings of peripheral primitive neuroectodermal tumors. Acta Radiol. 2015;56:820–8.
22. Seo JM, Park BK, Park SY, Kim CK. Characterization of lipid-poor adrenal adenoma: chemical-shift MRI and washout CT. Am J Roentgenol. 2014;202:1043–50.
23. Zhang YM, Lei PF, Chen MN, Lv XF, Ling YH, Cai PQ, et al. CT findings of adrenal schwannoma. Clin Radiol. 2016;71:464–70.
24. Mannelli M, Colagrande S, Valeri A, Parenti G. Incidental and metastatic adrenal masses. Semin Oncol. 2010;37:649–61.